THE JOURNAL OF BIOLOGICAL CHEMISTRY VOL. 287, NO. 11, pp. 8126–8134, March 9, 2012

Resolving Holliday Junctions with *Escherichia coli* UvrD Helicase*

Received for publication, October 14, 2011, and in revised form, January 17, 2012 Published, JBC Papers in Press, January 21, 2012, DOI 10.1074/jbc.M111.314047

Annamarie S. Carter[‡§1,2], **Kambiz Tahmaseb**[‡1], **Sarah A. Compton**[¶3], **and Steven W. Matson**[‡4]

From the Departments of [‡]*Biology and* [§]*Chemistry and the* [¶]*Lineberger Comprehensive Cancer Center, University of North Carolina, Chapel Hill, North Carolina 27599*

Background: The ability of UvrD, a DNA helicase, to unwind a Holliday junction has not been directly tested.
Results: UvrD catalyzed robust unwinding of a Holliday junction producing a forked structure.
Conclusion: UvrD unwinds a Holliday junction by binding to the junction and translocating along opposite arms.
Significance: This result is likely to have relevance in recombination and replication.

The *Escherichia coli* UvrD helicase is known to function in the mismatch repair and nucleotide excision repair pathways and has also been suggested to have roles in recombination and replication restart. The primary intermediate DNA structure in these two processes is the Holliday junction. UvrD has been shown to unwind a variety of substrates including partial duplex DNA, nicked DNA, forked DNA structures, blunt duplex DNA and RNA-DNA hybrids. Here, we demonstrate that UvrD also catalyzes the robust unwinding of Holliday junction substrates. To characterize this unwinding reaction we have employed steady-state helicase assays, pre-steady-state rapid quench helicase assays, DNaseI footprinting, and electron microscopy. We conclude that UvrD binds initially to the junction compared with binding one of the blunt ends of the four-way junction to initiate unwinding and resolves the synthetic substrate into two double-stranded fork structures. We suggest that UvrD, along with its mismatch repair partners, MutS and MutL, may utilize its ability to unwind Holliday junctions directly in the prevention of homeologous recombination. UvrD may also be involved in the resolution of stalled replication forks by unwinding the Holliday junction intermediate to allow bypass of the blockage.

UvrD, a superfamily I helicase in *Escherichia coli*, has well documented roles in two important DNA repair pathways: methyl-directed mismatch repair and nucleotide excision repair (1–5). In the mismatch repair pathway UvrD initiates unwinding at the d(GATC)-located nick created by MutH and, together with an appropriate exonuclease, facilitates removal of the unmethylated daughter strand containing the mismatch (2, 6). UvrD also participates in the UvrABC nucleotide excision repair pathway by removing the 12–13-base oligonucleotide containing a pyrimidine dimer or bulky adduct (3). Additional functions for UvrD have been proposed, consistent with the pleiotropic nature of *uvrD* mutants (4, 5, 7), including roles in replication and recombination (8–12). The precise molecular role of UvrD in these processes is less clear although several possibilities have been suggested, and this is an area of active investigation.

Recent studies indicate that UvrD has a direct role in recombination reactions associated with replication fork rescue (13–15). Specifically, UvrD is required for regression of the nascent leading and lagging strands at a stalled replication fork leading to the formation of a Holliday junction (HJ)[5] (16, 17). The role played by UvrD has been the subject of intense study because it is now clear that replication fork restart is critical to maintaining genome stability (13, 15, 16, 18). Current models suggest that UvrD removes RecA assembled on single-stranded DNA (ssDNA) at a blocked replication fork to allow replication fork reversal to occur (15). This is consistent with *in vitro* experiments that have shown UvrD to be capable of removing RecA molecules from DNA thereby disrupting a recombination event (9, 18, 18, 19). It has also been suggested that UvrD could act to resolve the intermediate formed by replication fork regression so that the lesion may be repaired or bypassed immediately (16, 20).

UvrD has also been suggested to play a role in the prevention or correction of unwanted recombination events (21). Genetic experiments have shown that Δ*uvrD* mutants have a hyperrecombination phenotype, suggesting that UvrD may play a role in resolving the crossover intermediate (22, 23). Consistent with this idea, a hyporecombination phenotype is observed in a strain capable of overproducing UvrD (4, 11). In addition, genetic studies suggest that UvrD is involved in the MutH-independent homeologous recombination editing pathway along with MutS and MutL (24). Taken together, these data suggest the possibility that UvrD might recognize and unwind a HJ structure.

Previous studies using the purified protein have shown that UvrD translocates unidirectionally along the DNA lattice with a 3′ to 5′ polarity and preferentially unwinds DNA substrates with a 3′-ssDNA overhang (25, 26). UvrD has also been shown

* The work was supported, in whole or in part, by National Institutes of Health Grant GM33476 (to S. W. M.).
[1] Both authors contributed equally to this work.
[2] Present address: Dept. of Biochemistry and Molecular Biology, Virginia Commonwealth University, Richmond, VA.
[3] Present address: ZenBio, 3200 East Hwy. 54, Suite 100, Research Triangle Park, NC.
[4] To whom correspondence should be addressed: Dept. of Biology, CB 3280, Coker Hall, University of North Carolina, Chapel Hill, NC 27599-3280. Tel.: 919-962-0005; Fax: 919-962-1625; E-mail: smatson@bio.unc.edu.

[5] The abbreviations used are: HJ, Holliday junction; AMP-PNP, adenosine 5′-(β,γ-imino)triphosphate; ATPγS, adenosine 5′-*O*-(thiotriphosphate).

TABLE 1
Oligonucleotides used to create synthetic substrates for this study

Oligonucleotide name	Length	Sequences from 5′ to 3′
	nucleotides	
X12-1	50	GAC GCT GCC GAA TTC TGG CTT GCT AGG ACA TCT TTG CCC ACG TTG ACC CG
X12-2	50	CGG GTC AAC GTG GGC AAA GAT GTC CTA GCA ATG TAA TCG TCT ATG ACG TC
X12-3	50	GAC GTC ATA GAC GAT TAC ATT GCT AGG ACA TGC TGT CTA GAG ACT ATC GC
X12-3 3′ overhang	80	GAC GTC ATA GAC GAT TAC ATT GCT AGG ACA TGC TGT CTA GAG ACT ATC GCT TTT TTT TTT TTT TTT TTT TTT TTT TTT TT
X12-4	50	GCG ATA GTC TCT AGA CAG CAT GTC CTA GCA AGC CAG AAT TCG GCA GCG TC
X3-1	40	ACC TGA GAG CAG TCA ACG TGC CGA GCC GCG TGT CGG ATT T
X3-2	41	AAA TCC GAC ACG CGG CTC GGC AAG CTA CGT ACC GAA TCT CG
X3-3	41	CGA GAT TCG GTA CGT AGC TTG CTA CGG AAT GGC TAC GTA GC
X3-4	40	GCT ACG TAG CCA TTC CGT AGC ACG TTG ACT GCT CTC AGG T
K1	55	ATC GAT AGT CTC TAG ACA GCA TGT CCT AGC AAG CCA GAA TTC GGC AGC GTC AGC C
K2	54	GAC GCT GCC GAA TTC TGG CTT GCT AGG ACA TCT TTG CCC ACG TTG ACC CAA GCC
K3	55	TGG GTC AAC GTG GGC AAA GAT GTC CTA GCA ATG TAA TCG TCT ATC ACG TTG AGC C
K4	56	CAA CGT CAT AGA CGA TTA CAT TGC TAG GAC ATG CTG TCT AGA GAC TAT CGA TAG CC

to unwind nicked and blunt duplex DNA, albeit at higher protein concentrations (27). In addition, UvrD is able to recognize and unwind a variety of forked DNA structures (28, 29). However, the unwinding of a HJ, the presumed DNA intermediate in replication restart and recombination, has not been investigated. We have examined this possibility here using multiple synthetic junctions ranging in overall size, extent of the mobile junction, and other characteristics.

The data indicate that UvrD is capable of recognizing and unwinding synthetic HJ substrates with the initial product being a two-stranded forked DNA structure. To characterize this unwinding reaction two different binding and unwinding mechanisms were considered. The first mechanism posits UvrD binding to one of the blunt ends on the four-armed structure and unwinding a single oligonucleotide at a time. The second mechanism proposes UvrD binding to the center of the structure, likely as a dimer, and effectively pulling opposite strands into the junction creating two double-stranded forked DNA structures. A second event would then be necessary for a single-stranded species to be observed. We used several biochemical and physical methods to demonstrate that UvrD binds to the center of the HJ structure and resolves the junction through a double-stranded DNA intermediate.

EXPERIMENTAL PROCEDURES

DNA Substrates—Three synthetic HJ substrates were constructed using purified oligonucleotides (Integrated DNA Technologies) (Table 1). For each junction one of the oligonucleotides was labeled on the 5′ end with [γ-^{32}P]ATP (Perkin-Elmer Life Sciences) using T4 polynucleotide kinase (New England Biolabs) under supplier-recommended conditions. The [^{32}P]DNA oligonucleotide was separated from [γ-^{32}P]ATP using a Sephadex G-50 spin column (Pharmacia) equilibrated with 10 mM Tris-HCl (pH 7.5)/0.1 mM EDTA (TE) and then annealed to the three other oligonucleotides at a four to one excess of unlabeled oligonucleotides to labeled DNA. For HJ X12, oligonucleotides X12-1, X12-2, X12-3, and X12-4 were annealed. For the HJ X12 junction with a 3′-ssDNA overhang, oligonucleotides X12-1, X12-2, and X12-3 with a 30-nucleotide poly(dT) 3′-ssDNA tail, and labeled X12-4 were annealed. For HJ X3, oligonucleotides X3-1, X3-2, X3-3, and X3-4 were annealed. Annealing reactions were performed in annealing buffer containing 50 mM Tris-HCl (pH 7.5), 50 mM NaCl, 10 mM MgOAc, and 5 mM dithiothreitol (DTT). The temperature of the annealing mixture was increased to 95 °C and then slow cooled to room temperature. After annealing, the HJ structures were purified by electrophoresis on a native 10% polyacrylamide gel, electroeluted in 1× TBE (89 mM Tris/89 mM borate/1 mM EDTA) with 10 mM $MgCl_2$ overnight at 120 V and dialyzed against TEN buffer (50 mM NaCl, 10 mM Tris-HCl (pH 8.0), and 0.1 mM EDTA) for 2 h. The final DNA concentration was determined based on counts per minute (cpm) after dialysis *versus* cpm measured off the G-50 column. We estimated a 95% recovery of labeled single-stranded oligonucleotide from the G-50 column for these calculations.

The HJ used for EM analysis was constructed as described previously (30, 31). Briefly, the HJ was constructed by annealing four oligonucleotides resulting in a small four-way HJ with 5′-AGCC-3′ overhangs at each end. These junctions were converted into larger HJ substrates suitable for visualization with EM by ligation of four 575-bp double-stranded DNA arms onto the junction. DNA molecules containing all four arms were gel-purified prior to use.

Protein Purification—UvrD was purified as described previously (32).

Helicase Assays—All unwinding reactions (20 μl) were executed in UvrD reaction buffer (25 mM Tris-HCl (pH 7.5), 4 mM $MgCl_2$, 5 mM β-mercaptoethanol, 20 mM NaCl, and 0.2 mg ml^{-1} BSA). 0.1 nM HJ [^{32}P]DNA was incubated with varying concentrations of UvrD, diluted in UvrD storage buffer (20 mM Tris-HCl (pH 8.3), 200 mM NaCl, 50% glycerol, 1 mM EDTA, 0.5 mM EGTA, 15 mM β-mercaptoethanol), at 37 °C for 5 min before initiating the reaction with the addition of ATP to a final concentration of 3 mM. Reactions were incubated for 5 min at 37 °C and stopped with a 3× helicase stop solution (final concentration 10% glycerol, 16.7 mM EDTA, 0.5× TBE, 0.1% SDS, 0.02% xylene cyanol/bromphenol blue) containing an excess of unlabeled oligonucleotide corresponding to the [^{32}P]DNA oligonucleotide in the substrate. Immediately after adding stop solution the samples were placed on ice. The reaction products were analyzed by gel electrophoresis using a 10% native polyacrylamide gel containing 0.1% SDS. The gels were electrophoresed at 200 V for 2.5 h. Results were visualized using a Storm 840 PhosphorImager (Molecular Dynamics) and quantified using

ImageQuant software (Molecular Dynamics). SigmaPlot (Jandel Scientific) was used for graphing results.

Rapid Quench—Rapid quench-flow analysis of HJ unwinding by UvrD was performed using a KinTek quench-flow apparatus model RQF-3 (KinTek Corp). One syringe contained a mixture of 1× reaction buffer, 50 nM UvrD, and 2 nM DNA substrate. The other syringe contained 1× UvrD reaction buffer and 6 mM ATP. The two parts of the reaction were mixed separately on ice and allowed to incubate for 15 min. The tubes were then incubated at room temperature (20 °C) for 5 min followed by loading each mixture into the appropriate loops of the quench-flow apparatus. The two halves of the reaction were mixed rapidly and quenched using a solution that contained 200 mM EDTA, 0.2% SDS, and 20 nM cold competitor oligonucleotide to prevent reannealing of the labeled oligonucleotide. 20 μl of each time point was mixed with 5 μl of 5× loading buffer (50% glycerol, 2.5× TBE, and 0.05% xylene cyanol and bromphenol blue) and loaded onto 10% polyacrylamide gels containing 0.5× TBE and 0.1% SDS. The results were visualized using the Storm 840 PhosphorImager.

DNaseI Footprinting Assays—All footprinting reaction mixtures (10 μl) contained 25 mM Tris-HCl (pH 7.5), 4 mM $MgCl_2$, 5 mM β-mercaptoethanol, 20 mM NaCl, 0.2 mg ml^{-1} BSA, 0.4 nM HJ (X3, X12, or X12 3′-overhang as indicated), 3 mM AMP-PNP, and UvrD (as indicated). Reactions were incubated for 15 min at 37 °C, to allow binding of UvrD, prior to the addition of 1 mM $CaCl_2$ and 5 μg ml^{-1} DNaseI. Incubation was continued at 37 °C for 4 min. Reactions were terminated by adding 10 μl of a stop solution containing 90% formamide, 0.05% bromphenol blue, 0.05% xylene cyanol, and 25 mM EDTA. Samples were boiled for 5 min and resolved on a 16% denaturing polyacrylamide gel containing 7 M urea. Results were imaged using a Storm 840 PhosphorImager.

Preparation of Samples for EM—UvrD (1.5 μg ml^{-1}; 16 nM) was incubated with the large HJ substrate (0.5 μg ml^{-1}; 0.3 nM) for 5 min at 37 °C in reaction mixtures (30 μl) containing 25 mM Tris-HCl (pH 7.6), 3 mM $MgCl_2$, 20 mM NaCl, 5 mM DTT, and 3 mM ATPγS. Protein-DNA complexes were fixed with 0.6% glutaraldehyde for 5 min at room temperature; excess glutaraldehyde and binding buffer components were diluted with two reaction volumes of 10 mM Tris-HCl (pH 7.6) and 0.1 mM EDTA prior to EM.

Electron Microscopy—DNA-bound protein samples were individually mixed with a buffer containing 2.5 mM spermidine (33) and incubated on glow-charged carbon foil grids for 3 min. Samples were washed with a series of water-ethanol washes, air-dried, and rotary shadowcast with tungsten at 1×10^{-6} torr. Samples were analyzed using a Tecnai 12 transmission electron microscope (FEI) at 40 kV, and images were captured on a Gatan Ultrascan 4000 slow scan CCD camera and supporting software (Gatan Inc.). Image size and contrast were adjusted using Adobe Photoshop.

RESULTS

UvrD has well established roles as a DNA helicase in both methyl-directed mismatch repair and excision repair (2, 3, 6, 34–36). In addition, genetic and biochemical studies suggest the possibility of roles in recombination and DNA replication (8–12, 22). However, these roles are not well defined. The HJ is a primary intermediate DNA structure in recombination and in recombination-mediated replication restart. Here, we have characterized the ability of UvrD to unwind synthetic HJ substrates.

Helicase Activity on HJ Substrate—To determine whether UvrD could resolve a HJ, unwinding reactions were performed using several synthetic HJ DNA substrates including the X12 junction described by Elborough and West (37) and a modification of this substrate that has reduced mobility at the junction (X3). These substrates differ in two primary characteristics: the mobility of the junction and the length of the arms. HJ X12 has a 12-nucleotide region of homology at the center of the junction and 25-bp arms whereas HJ X3 has only 3 nucleotides of homology at the center of the junction and slightly shorter, 20-bp, arms. Each substrate was constructed by annealing the appropriate four oligonucleotides and the substrate was purified as detailed under "Experimental Procedures." The DNA sequence for each of the oligonucleotides used to construct these substrates is listed in Table 1.

UvrD catalyzed robust unwinding of both synthetic HJ substrates (Fig. 1) in a reaction dependent on ATP hydrolysis (data not shown). Essentially complete unwinding of each substrate was achieved with 10–20 nM UvrD in a 5-min incubation (Fig. 1, *A* and *C*). Importantly, the primary unwound product observed at low concentrations of UvrD was a two-stranded fork structure as indicated by quantification of each product of the unwinding reaction as a function of protein concentration (Fig. 1, *B* and *D*). At higher concentrations of UvrD the substrate was completely unwound to yield ssDNA product. We observed no significant accumulation of three-stranded product in these UvrD titrations. This suggests that the mechanism used by UvrD to unwind the HJ DNA goes through a two-stranded intermediate. The significance of this observation will be discussed below.

In the experiments using the HJ X3 substrate a doublet was visible at the two-stranded fork structure position (Fig. 1*C*). This can be attributed to the length of oligonucleotides used to create the HJ X3 substrate (two 41-mers and two 40-mers). From these four oligonucleotides, there are four possible two-stranded combinations. They would consist of one 41/41-mer combination, two 41/40-mer combinations, and one 40/40-mer combination. Because the HJ X3 substrate is prepared by radioactive labeling of one oligonucleotide, X3-1, only two of these products would be visible. One of the doublet species would be the combination of a 41-mer and a 40-mer, the other would be two annealed 40-mers. There would also be two unlabeled species (a 41/41-mer and a different 41/40-mer).

Comparison of appropriate marker molecules with the products of the unwinding reaction confirmed that the doublet was the result of the two unwinding outcomes predicted above (data not shown). These observations are consistent with the notion that UvrD binds to the junction to initiate the unwinding reaction. One two-stranded product is the result of binding followed by pulling the left and right arms toward the center whereas the other two-stranded product is the result of binding followed by pulling the top and bottom arms toward the center. There is no apparent preference for one product over the other

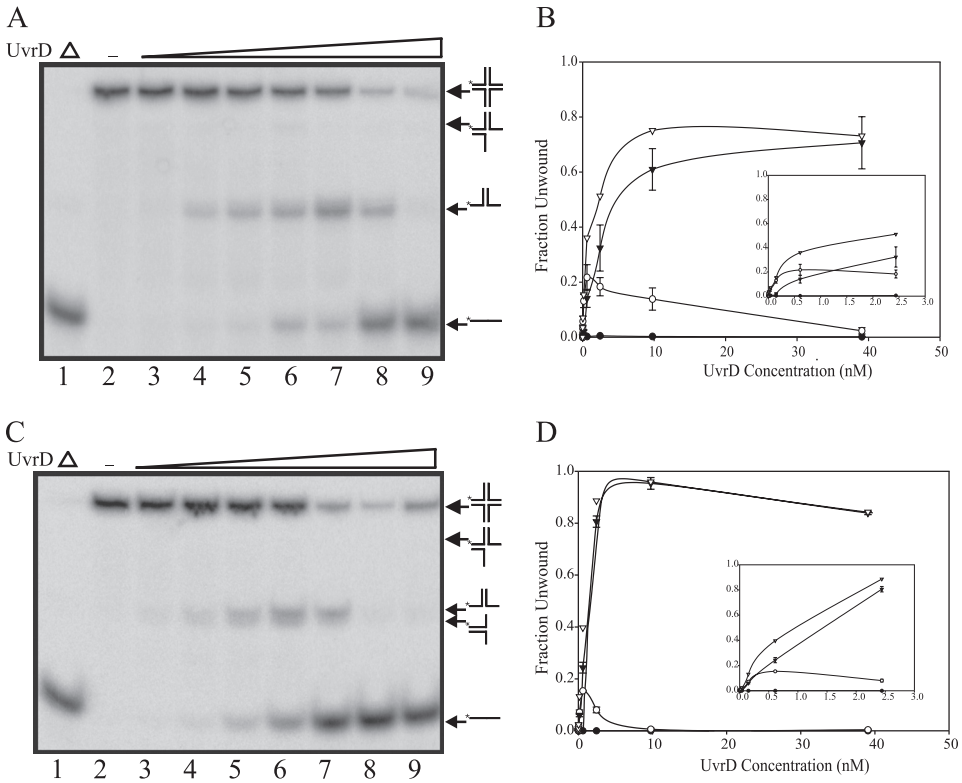

FIGURE 1. **UvrD unwinding of HJ substrates under steady-state conditions.** *A*, products of reactions containing 0.1 nM HJ X12 and increasing concentrations of UvrD (*lane 1*, heat denatured control; *lane 2*, no protein; *lane 3*, 9.5 pM UvrD; *lane 4*, 38 pM UvrD; *lane 5*, 150 pM UvrD; *lane 6*, 610 pM UvrD; *lane 7*, 2.44 nM UvrD; *lane 8*, 9.77 nM UvrD; and *lane 9*, 39.1 nM UvrD) resolved on a native polyacrylamide gel. The substrate and possible unwinding products are depicted on the *right*. *B*, quantification of the HJ X12 unwinding products as a function of UvrD concentration. The data from at least three independent experiments were quantified; three-stranded structure (●), two-stranded structure (○), single-stranded oligonucleotide (▼), and total unwinding (▽). The *inset* is a magnified view of the plot at UvrD concentrations up to 2.5 nM. *C*, products of reactions containing 0.1 nM HJ X3 and increasing concentrations of UvrD (lane order and protein concentrations are identical to *A*) resolved on a native polyacrylamide gel. The substrate and possible unwinding products are depicted on the *right*. *D*, quantification of the HJ X3 unwinding products as a function of UvrD concentration. The data from at least three independent experiments were quantified. The *symbols* used to denote each structure are the same as in *B*. UvrD concentrations are expressed as monomer protein, and *error bars* represent ± S.E.

as evidenced by the equivalent accumulation of each possible two-stranded product.

Helicase Activity under Rapid Quench Conditions—To provide additional evidence for initiation of the unwinding reaction at the junction, we performed rapid quench kinetic experiments. This allowed analysis of the initial product formed in unwinding reactions using HJ substrates. Two substrates were used in these experiments, the HJ X3 substrate used in the experiments shown in Fig. 1*C* and HJ X12 substrate modified to include a 30-nucleotide poly(dT) 3′-ssDNA tail on one arm. We reasoned that HJ X12 with a 30-nucleotide 3′-ssDNA tail on one arm would allow binding of UvrD to the 3′-ssDNA overhang. This would allow observation of the three-stranded intermediate because a 3′-ssDNA tail is a preferred substrate for UvrD (25, 27) providing a good comparison with the HJ X3 substrate with fully duplex DNA arms.

Rapid quench kinetic studies of unwinding of the X3 substrate demonstrated the formation of the two-stranded intermediate with almost no formation of the three-stranded product (Fig. 2*A*) in the initial time points, as was observed in the steady-state experiments (see Fig. 1*C*). However, as anticipated, the three-stranded structure was observed first, followed by a reduced amount of the two-stranded product and a small amount of ssDNA product, using the HJ X12 substrate with a ssDNA 3′-ssDNA tail (Fig. 2*B*). This indicates that UvrD can bind one arm of the substrate to initiate unwinding and produce a three-stranded structure and a ssDNA product when a binding site with high affinity is provided.

Taken together, these data demonstrate that unwinding by UvrD can produce the expected three-stranded product when UvrD is induced to bind at the end of one arm of the substrate by the addition of a ssDNA tail. However, in the absence of this tail UvrD preferentially binds the junction to initiate unwinding with the production of a two-stranded intermediate.

These results suggest that UvrD catalyzes the robust unwinding of a HJ substrate by binding, presumably as a dimer, to the junction and then translocating along opposite arms of the junction to yield a two-stranded structure (Fig. 3*A*). This result was, perhaps, unexpected because UvrD has been shown to be capable of initiating an unwinding reaction at a blunt end (28, 38). If UvrD were initiating the unwinding of the HJ substrate at one of the blunt ends then we would have expected to observe significant accumulation of a three-stranded product (Fig. 3*B*). Although we do observe the production of a small amount of three-stranded product (see Fig. 2*B*), this is significantly reduced relative to the accumulation of the two-stranded product (Fig. 1, *B* and *D*). As expected, the two-stranded product is a substrate for UvrD and is unwound to yield the ssDNA product ultimately observed in unwinding reactions at higher UvrD concentrations. This suggests that UvrD has a higher affinity

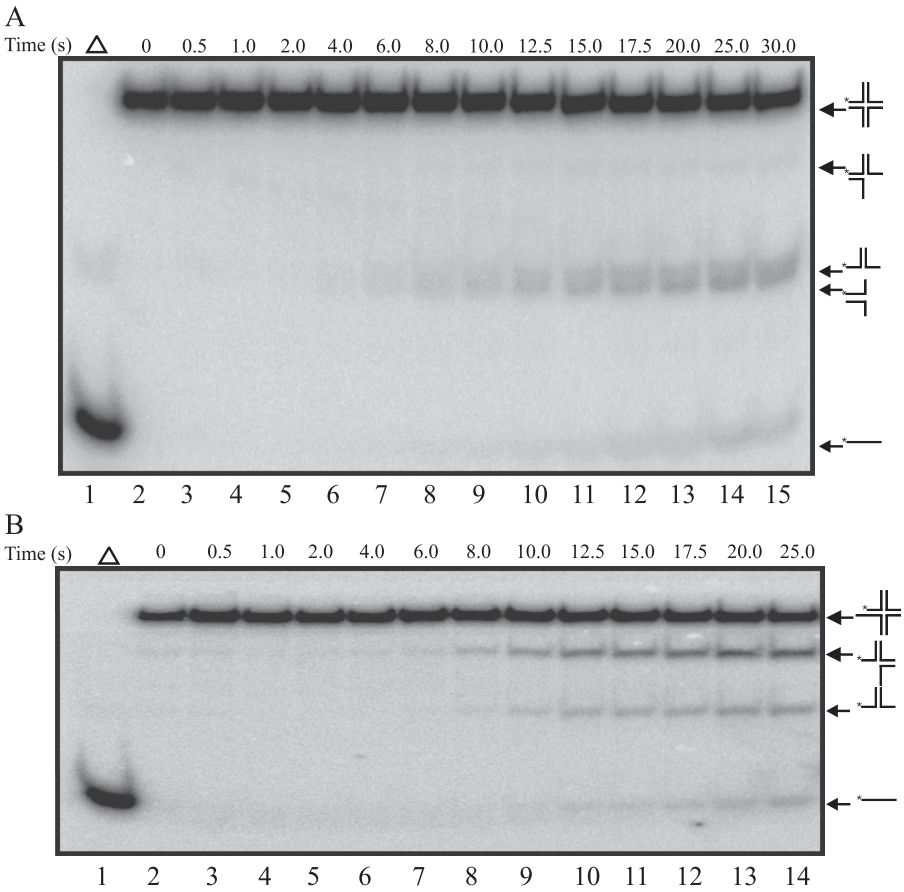

FIGURE 2. **Pre-steady-state rapid quench kinetic analysis of HJ unwinding.** *A*, reactions containing 25 nM UvrD and 1 nM HJ X3 were as described under "Experimental Procedures" and resolved on a native polyacrylamide gel. The time points ranged from 0.5 to 30 s as indicated. The substrate and possible unwinding products are depicted on the *right*. *B*, reactions containing 25 nM UvrD and 1 nM HJ X12 with a 30 nucleotide poly(dT) 3′ tail were as described under "Experimental Procedures" and resolved on a polyacrylamide gel. The time points ranged from 0.5 to 25 s as indicated. The substrate and possible unwinding products are depicted on the *right*.

for the junction in the HJ X3 and HJ X12 substrates than for the blunt-ended duplex DNA arms.

DNaseI Footprinting of UvrD on HJ Substrates—To provide additional evidence for the binding of UvrD to the junction, DNaseI footprinting was used to define the initial binding site of UvrD on a HJ substrate in the presence of a nonhydrolyzable ATP analog. DNaseI footprints using both HJ substrates HJ X12 (data not shown) and HJ X3 were completed. Binding to HJ X3 was easier to visualize, perhaps due to restricted migration at the junction, and is shown in Fig. 4*A*. As the concentration of UvrD was increased, there was an obvious decrease in available dsDNA for DNaseI to cleave. The position of the bound UvrD protein centers near the 22-nucleotide marker consistent with binding to and protection of the junction. In addition, we tested the ability of purified RuvA to block access of UvrD to the junction. RuvA effectively inhibited unwinding of HJ X12 in a concentration-dependent manner (data not shown).

The HJ X12 substrate with a 30-nucleotide poly(dT) 3′-ssDNA tail was also used as a substrate in DNaseI footprinting studies. The preferred binding site for UvrD on this substrate should be at the site of the ssDNA overhang, consistent with the unwinding assay results presented above. In Fig. 4*B*, the site of the 3′ single-strand–double-strand junction corresponds to the labeled 5′ end of oligonucleotide X12-4. Therefore, binding to the single-strand–double-strand junction would block DNaseI cleavage of the 5′ end of the labeled DNA strand. The DNaseI digestion pattern indicates that UvrD is, in fact, binding to the end of this structure and is comparatively different from the footprint seen on HJ X3 where UvrD is bound to the junction. The last lane (high concentration of UvrD) in both panels shows an apparent loss of DNaseI cleavage along the length of the [^{32}P]DNA oligonucleotide. This is most likely due to the high concentration of UvrD.

Visualization of UvrD Binding to HJ Substrates by EM—EM was used to visualize the binding of UvrD to large HJ DNAs directly. The HJ substrate used for EM was similar to the substrates used for biochemical assays. It contained a mobile junction of 12 nucleotides in length but was constructed with long (575-bp) arms to make it suitable for visualization by EM.

UvrD was incubated with the HJ DNA in the presence of a poorly hydrolyzed ATP analog to prevent unwinding, fixed, and adsorbed onto carbon supporting grids, and then shadowcast with tungsten as described under "Experimental Procedures." DNA molecules were arbitrarily counted from four individual experiments. Of the 529 molecules scored, UvrD bound 72 ± 8% of the HJ substrates. UvrD was visualized specifically at the four-way junction in 93 ± 4% of the protein-bound molecules (72 ± 14% of all DNA molecules counted) (Fig. 5, *upper*, *A*–*G*). Interestingly, some of the molecules were observed with one of

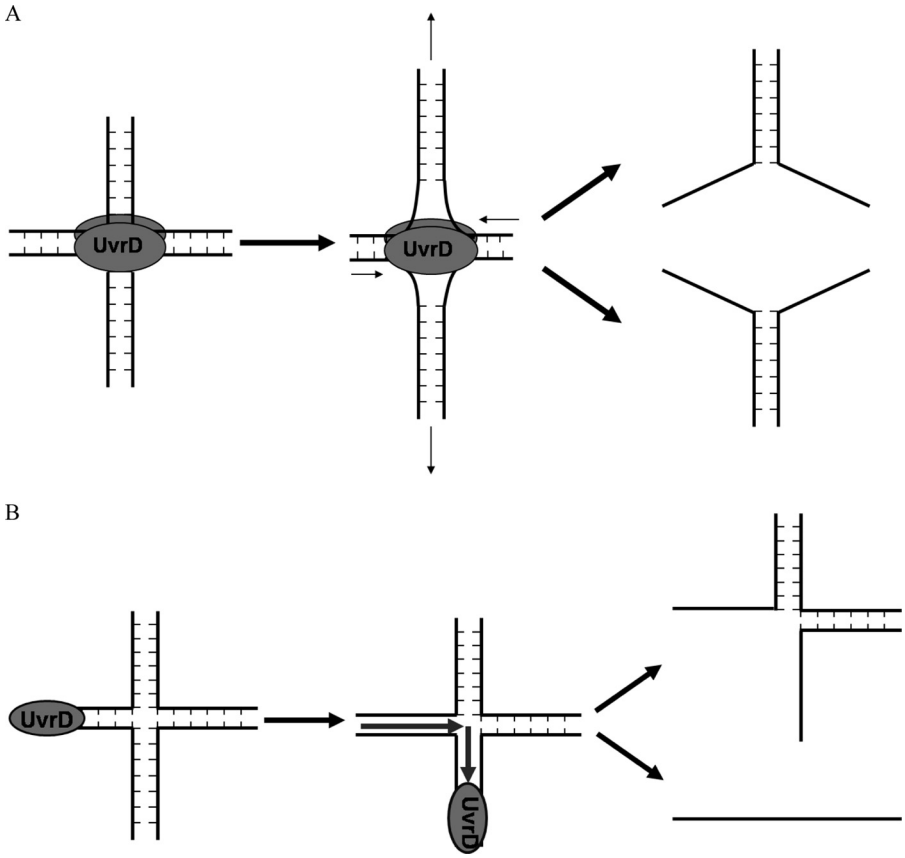

FIGURE 3. **Two models for HJ unwinding by UvrD.** *A*, UvrD binds to the mobile crossover site, presumably as a dimer, and initiates unwinding by translocating along opposite arms (as shown by *thin arrows*) to yield two two-stranded structures. A second unwinding event (not shown) would then be necessary to produce all four single oligonucleotides. *B*, UvrD binds to a blunt end and translocates along one strand to yield a three-stranded forked structure and a single-stranded oligonucleotide.

the HJ arms looping back into the center of the junction with UvrD protein observed at the junction center (Fig. 5, *upper*, *D–G*). The majority (51 ± 14%) of the junction-bound molecules did not exhibit this looped structure. However, 32 ± 9% of the junction-bound molecules were bound with one arm looped in toward the junction (Fig. 5, *upper*, *D–F*), and 9 ± 9% molecules were bound at the junction with more than one looped arm (Fig. 5, *upper*, G). There was also a small fraction (7 ± 4%) of the bound substrates with protein localized at sites other than the junction. Of these molecules, 4 ± 3% were bound at the blunt end of the DNA (Fig. 5, *upper*, *H*), and the rest (3 ± 3%) were bound internally between the junction and the end of the arm (Fig. 5, *upper*, *I*). In addition, we occasionally observed multiple HJ DNAs bound by a single large protein complex that likely results from aggregation of protein-bound DNA molecules. These data indicate a remarkably high preference of UvrD for binding to the alternate secondary structure (*i.e.* the HJ) relative to the much longer regions of duplex B-form DNA or blunt ends.

DISCUSSION

Purified UvrD has been shown to unwind a wide variety of DNA substrates including partial duplex DNAs, blunt-ended substrates, nicked DNA, and synthetic fork structures representing various possibilities at a blocked replication fork (25, 27, 29, 39, 40). In addition, UvrD has been shown to unwind RNA-DNA hybrids (41) as well as displacing RecA bound to ssDNA (9, 19). The promiscuous unwinding activity of UvrD is likely a reflection of its multiple roles in the cell including roles in repair, replication, and recombination consistent with the pleiotropic phenotype of *uvrD* mutants (1).

Based on the data presented here, we suggest that UvrD also recognizes and unwinds a HJ substrate by the general mechanism shown in Fig. 3*A*. When the synthetic HJ contains fully duplex arms UvrD preferentially binds to the mobile junction, presumably as a dimer, to initiate unwinding. Several lines of evidence support this conclusion including rapid quench kinetic studies, DNaseI footprinting, and direct visualization of UvrD binding to the HJ using EM. Subsequent to the binding event, UvrD resolves the HJ substrate into two double-stranded fork structures by translocating along opposite arms until the end of the arms is reached. This is similar to the mechanism used by RuvAB to migrate HJs prior to resolution of the junction by RuvC (42). The intermediate double-stranded fork structures are themselves substrates for UvrD and, thus, the final product of this *in vitro* reaction is ssDNA.

The salient features of the reaction we have described include the preferential binding of UvrD to the mobile junction and the ability of the UvrD dimer to either unwind or migrate this junction. Initial binding of UvrD to the junction was demonstrated using DNaseI footprinting assays which showed UvrD bound at

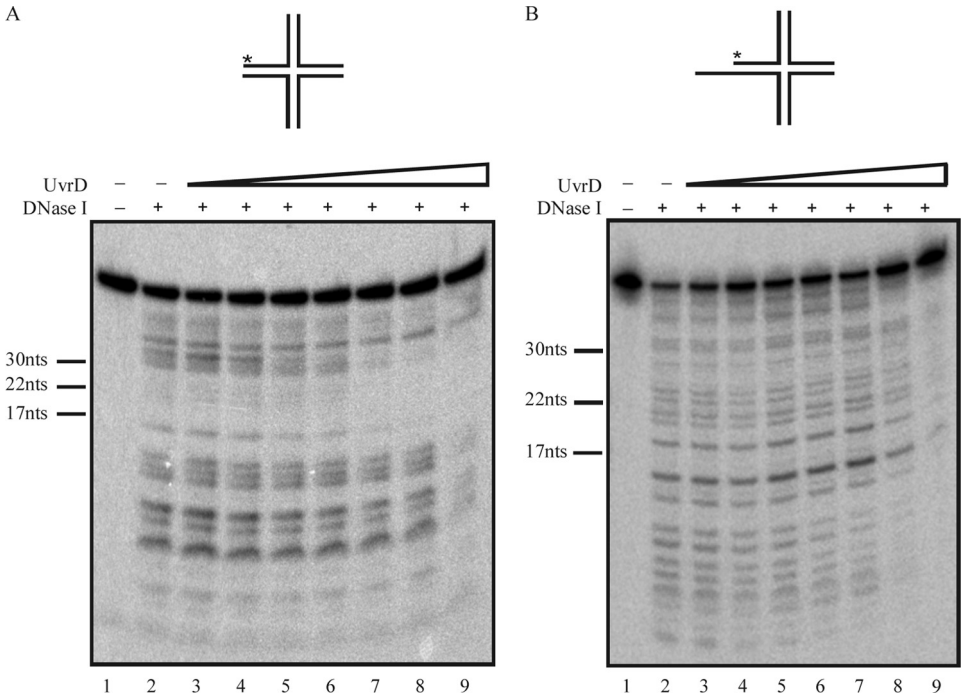

FIGURE 4. **DNaseI footprints of UvrD binding on HJ X3 and HJ X12-3′ overhang.** Reaction mixtures containing 0.4 nM HJ DNA were incubated with UvrD concentrations ranging from 0.2 to 104 nM as described under "Experimental Procedures." DNaseI (5 μg ml^{-1}) was added to the reactions shown in *lanes 2–8* of *A* and *B*. *Lanes 1* and *2* represent a no-protein control sample and a no-UvrD control, respectively. Reaction products were resolved on a denaturing polyacrylamide gel. *A*, footprint of UvrD on HJ X3. *B*, footprint of UvrD on HJ X12 with 3′ overhang. The positions of labeled oligonucleotide markers with lengths of 17, 22, and 30 nucleotides are shown on the *left*.

the junction in the presence of a poorly hydrolyzed analog of ATP to prevent unwinding. When the analysis was extended to a synthetic HJ substrate containing a 3′-ssDNA overhang, we observed UvrD bound on the ssDNA end as expected based on the preference of this protein for binding to ssDNA (39, 40). Direct visualization of UvrD bound on a HJ substrate DNA by EM confirmed the DNaseI footprinting studies and showed that at a typical concentration used in biochemical assays (16 nM), UvrD exhibits a high preference for the HJ structure. The smaller junction used as a base for the larger HJ structure in the EM experiments has a 12-nuceotide region of homology similar to that in X12. Very few protein molecules were observed binding to blunt ends of the structure or along the double helical arms consistent with our interpretation of the biochemical data. It should be noted that the concentration of blunt ends and duplex DNA is much higher than the concentration of the HJ structure. This indicates that the affinity of UvrD for the junction structure is significantly higher than its affinity for either duplex DNA or blunt-ended DNA.

Interestingly, a subset of the junction-bound molecules was visualized with a looping characteristic where the end of one arm was brought into the junction. In looped molecules the protein complex appears larger than in molecules with UvrD bound at the junction but not looped. Initially, we hypothesized that UvrD would bind as a dimer to the HJ, but perhaps it may also function as a dimer of dimers with one dimer bound to the junction and another dimer bound at a blunt end arm. UvrD has been shown to function as a dimer (43), and an association of UvrD molecules has been visualized through EM supporting this possibility (44).

Rapid quench kinetic experiments showed a clear difference when the unwinding products of the X3 HJ substrate and the X12 HJ substrate with an overhang were compared. When the ssDNA extension was present on one arm of the HJ substrate UvrD bound to that arm of the molecule and produced two products: a three-stranded structure and ssDNA. When the ssDNA tail was removed a two-stranded intermediate was observed before either single-stranded or three-stranded structures appeared as reaction products. The three-stranded products seen at later times can be explained by a small amount of UvrD binding to the blunt end, but the primary product of the unwinding reaction derives from initiation at the junction and supports the model presented in Fig. 3*A*. Taken together, the data indicate that the affinity of UvrD for the ssDNA tail is somewhat higher than its affinity for the HJ, which is greater than its affinity for a duplex DNA end. Importantly, UvrD is able to initiate an unwinding reaction after binding directly to the junction.

Other helicases in *E. coli* have been shown to unwind HJ substrates including RuvAB, DnaB, and RecG (42, 45–47). RuvAB is the archetypal HJ migrating helicase that, together with RuvC, participates directly in the late stages of homologous recombination (42). DnaB, the main replicative helicase in *E. coli* (48), is a hexameric helicase that has been proposed to bind a 5′-ssDNA overhang on one arm of a synthetic HJ structure and then, encircling the two strands of DNA, is able to migrate the junction to create a double-stranded product (45). UvrD functions as a dimer (49) and differs from DnaB mechanistically in that it binds directly to the junction to unwind the DNA leading to a double-stranded product. UvrD does not

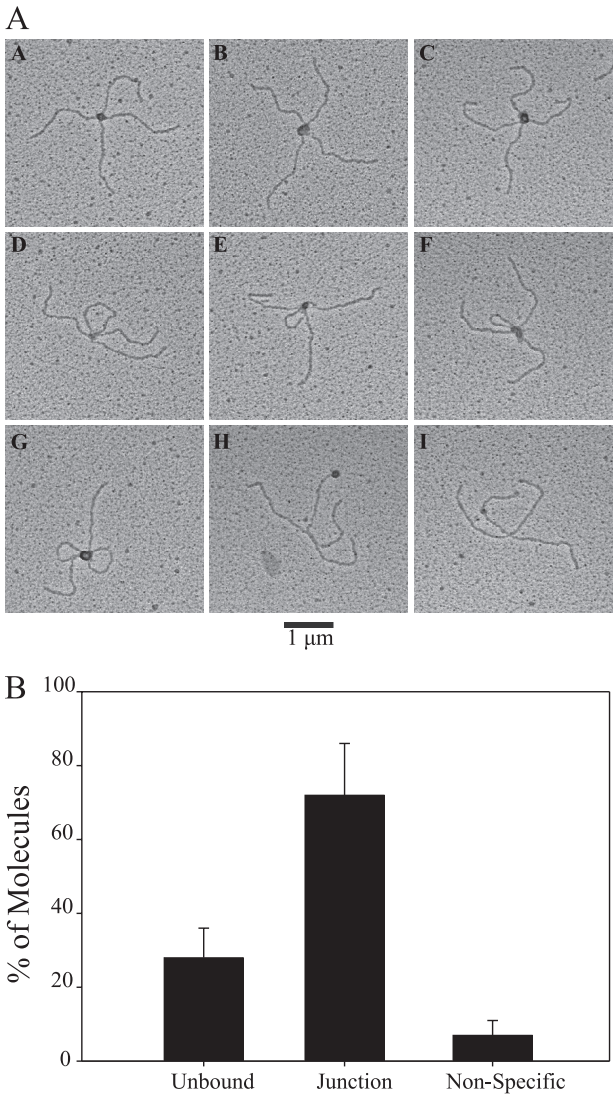

FIGURE 5. **Visualization of UvrD bound to HJ substrates by EM.** *Upper*, UvrD was incubated with HJ DNA templates, mounted onto carbon-coated copper grids, and rotary shadowcast with tungsten for visualization by EM as described under "Experimental Procedures." Representative individual molecules are shown. UvrD was observed bound specifically to the junction (*A–G*) with some molecules containing one or more looped arms (*D–G*) or bound nonspecifically at the end of an arm or along the arm itself (*H* and *I*). Images are shown in *reverse contrast*. *Scale bar*, 1 μm. *Lower*, quantitative analysis of UvrD binding to HJs is shown. DNA molecules ($n = 529$) were surveyed to determine protein-free and protein-bound HJ molecules. The protein-bound DNAs were scored for specific and nonspecific binding (defined as junction binding or binding elsewhere on the HJ DNAs). *Error bars* represent S.D.

require a ssDNA tail to initiate the unwinding reaction. RecG unwinds HJs by binding to the crossover site and unwinding to produce a two-strand product (47). However, RecG also uses its helicase activity to form HJs from stalled replication forks using its wedge structure to simultaneously unwind two duplex regions (50).

UvrD has been suggested to have a role in replication restart *in vivo* (15, 16, 20). At blocked replication forks the creation of a reversed replication fork with a HJ structure has been proposed when the nascent leading and lagging strands anneal. UvrD has been shown to participate in replication fork reversal, presumably by removing RecA bound to regions of ssDNA present at the blocked fork (18). We suggest that UvrD may also have a role in migrating or resolving the HJ formed at the reversed fork. It is also possible that UvrD may use its ability to self-associate as seen in the looped molecules observed in our EM experiments to recognize the shorter, recessed arm at a reversed replication fork and unwind the HJ structure in a guided, specific direction. Such an unwinding event would allow replication machinery to reload and bypass the lesion provided that additional nucleotides had been incorporated using the nascent lagging strand as a template (for review, see Ref. 17).

An alternative, but not mutually exclusive role for the HJ unwinding activity of UvrD has been suggested by the work of Stambuk and Radman (21) where UvrD is posited to be involved in the early stage prevention of unwanted recombination events, specifically in the case of preventing interspecies recombination. In this pathway, UvrD and its mismatch repair pathway partners, MutS and MutL, act to disrupt homeologous recombination independent of the activity of MutH. Disruption of the homeologous recombination event might involve MutS and MutL directing UvrD to the HJ and facilitating unwinding of the intermediate structure. Indeed, UvrD has been shown to interact with MutL, and its activity can be modulated by the interaction with MutL (2, 6). Additional work will be required to understand fully the significance of UvrD-catalyzed unwinding of HJ structures.

Acknowledgments—We thank Susan Whitfield for help with the figures and Jack Griffith for help with electron microscopy.

REFERENCES

1. Matson, S. W. (1991) DNA helicases of *Escherichia coli*. *Prog. Nucleic Acid Res. Mol. Biol.* **40,** 289–326
2. Iyer, R. R., Pluciennik, A., Burdett, V., and Modrich, P. L. (2006) DNA mismatch repair: functions and mechanisms. *Chem. Rev.* **106,** 302–323
3. Husain, I., Van Houten, B., Thomas, D. C., Abdel-Monem, M., and Sancar, A. (1985) Effect of DNA polymerase I and DNA helicase II on the turnover rate of UvrABC excision nuclease. *Proc. Natl. Acad. Sci. U.S.A.* **82,** 6774–6778
4. Maples, V. F., and Kushner, S. R. (1982) DNA repair in *Escherichia coli*: identification of the *uvrD* gene product. *Proc. Natl. Acad. Sci. U.S.A.* **79,** 5616–5620
5. Oeda, K., Horiuchi, T., and Sekiguchi, M. (1982) The *uvrD* gene of *E. coli* encodes a DNA-dependent ATPase. *Nature* **298,** 98–100
6. Matson, S. W., and Robertson, A. B. (2006) The UvrD helicase and its modulation by the mismatch repair protein MutL. *Nucleic Acids Res.* **34,** 4089–4097
7. Lundblad, V., and Kleckner, N. (1985) Mismatch repair mutations of *Escherichia coli* K12 enhance transposon excision. *Genetics* **109,** 3–19
8. Washburn, B. K., and Kushner, S. R. (1993) Characterization of DNA helicase II from a *uvrD252* mutant of *Escherichia coli*. *J. Bacteriol.* **175,** 341–350
9. Morel, P., Hejna, J. A., Ehrlich, S. D., and Cassuto, E. (1993) Antipairing and strand transferase activities of *E. coli* helicase II (UvrD). *Nucleic Acids Res.* **21,** 3205–3209
10. Bierne, H., Seigneur, M., Ehrlich, S. D., and Michel, B. (1997) *uvrD* mutations enhance tandem repeat deletion in the *Escherichia coli* chromosome via SOS induction of the RecF recombination pathway. *Mol. Microbiol.* **26,** 557–567
11. Petranović, M., Zahradka, K., Zahradka, D., Petranović, D., Nagy, B., Salaj-Smic, E., and Petranović, D. (2001) Genetic evidence that the elevated levels of *Escherichia coli* helicase II antagonize recombinational DNA repair. *Biochimie* **83,** 1041–1047

12. Mendonca, V. M., Kaiser-Rogers, K., and Matson, S. W. (1993) Double helicase II (*uvrD*)-helicase IV (*helD*) deletion mutants are defective in the recombination pathways of *Escherichia coli*. *J. Bacteriol.* **175,** 4641–4651
13. Michel, B., Boubakri, H., Baharoglu, Z., LeMasson, M., and Lestini, R. (2007) Recombination proteins and rescue of arrested replication forks. *DNA Repair* **6,** 967–980
14. Johnson, D. S., Bai, L., Smith, B. Y., Patel, S. S., and Wang, M. D. (2007) Single-molecule studies reveal dynamics of DNA unwinding by the ring-shaped T7 helicase. *Cell* **129,** 1299–1309
15. Lestini, R., and Michel, B. (2007) UvrD controls the access of recombination proteins to blocked replication forks. *EMBO J.* **26,** 3804–3814
16. Flores, M. J., Bidnenko, V., and Michel, B. (2004) The DNA repair helicase UvrD is essential for replication fork reversal in replication mutants. *EMBO Rep.* **5,** 983–988
17. Atkinson, J., and McGlynn, P. (2009) Replication fork reversal and the maintenance of genome stability. *Nucleic Acids Res.* **37,** 3475–3492
18. Florés, M. J., Sanchez, N., and Michel, B. (2005) A fork-clearing role for UvrD. *Mol. Microbiol.* **57,** 1664–1675
19. Veaute, X., Delmas, S., Selva, M., Jeusset, J., Le Cam, E., Matic, I., Fabre, F., and Petit, M. A. (2005) UvrD helicase, unlike Rep helicase, dismantles RecA nucleoprotein filaments in *Escherichia coli*. *EMBO J.* **24,** 180–189
20. Michel, B., Grompone, G., Florès, M. J., and Bidnenko, V. (2004) Multiple pathways process stalled replication forks. *Proc. Natl. Acad. Sci. U.S.A.* **101,** 12783–12788
21. Stambuk, S., and Radman, M. (1998) Mechanism and control of interspecies recombination in *Escherichia coli*. I. Mismatch repair, methylation, recombination and replication functions. *Genetics* **150,** 533–542
22. Zieg, J., Maples, V. F., and Kushner, S. R. (1978) Recombinant levels of *Escherichia coli* K-12 mutants deficient in various replication, recombination, or repair genes. *J. Bacteriol.* **134,** 958–966
23. Arthur, H. M., and Lloyd, R. G. (1980) Hyper-recombination in *uvrD* mutants of *Escherichia coli* K-12. *Mol. Gen. Genet.* **180,** 185–191
24. Radman, M., Matic, I., Halliday, J. A., and Taddei, F. (1995) Editing DNA replication and recombination by mismatch repair: from bacterial genetics to mechanisms of predisposition to cancer in humans. *Philos. Trans. R. Soc. Lond. B Biol. Sci.* **347,** 97–103
25. Matson, S. W. (1986) *Escherichia coli* helicase II (urvD gene product) translocates unidirectionally in a 3′ to 5′ direction. *J. Biol. Chem.* **261,** 10169–10175
26. Fischer, C. J., Maluf, N. K., and Lohman, T. M. (2004) Mechanism of ATP-dependent translocation of *E. coli* UvrD monomers along single-stranded DNA. *J. Mol. Biol.* **344,** 1287–1309
27. Runyon, G. T., and Lohman, T. M. (1989) *Escherichia coli* helicase II (UvrD) protein can completely unwind fully duplex linear and nicked circular DNA. *J. Biol. Chem.* **264,** 17502–17512
28. Runyon, G. T., and Lohman, T. M. (1993) Kinetics of *Escherichia coli* helicase II-catalyzed unwinding of fully duplex and nicked circular DNA. *Biochemistry* **32,** 4128–4138
29. Cadman, C. J., Matson, S. W., and McGlynn, P. (2006) Unwinding of forked DNA structures by UvrD. *J. Mol. Biol.* **362,** 18–25
30. Lee, S., Cavallo, L., and Griffith, J. (1997) Human p53 binds Holliday junctions strongly and facilitates their cleavage. *J. Biol. Chem.* **272,** 7532–7539
31. Compton, S. A., Tolun, G., Kamath-Loeb, A. S., Loeb, L. A., and Griffith, J. D. (2008) The Werner syndrome protein binds replication fork and holliday junction DNAs as an oligomer. *J. Biol. Chem.* **283,** 24478–24483
32. Runyon, G. T., Wong, I., and Lohman, T. M. (1993) Overexpression, purification, DNA binding, and dimerization of the *Escherichia coli uvrD* gene product (helicase II). *Biochemistry* **32,** 602–612
33. Griffith, J. D., and Christiansen, G. (1978) Electron microscope visualization of chromatin and other DNA-protein complexes. *Annu. Rev. Biophys. Bioeng.* **7,** 19–35
34. Lahue, R. S., Au, K. G., and Modrich, P. (1989) DNA mismatch correction in a defined system. *Science* **245,** 160–164
35. Matson, S. W., Bean, D. W., and George, J. W. (1994) DNA helicases: enzymes with essential roles in all aspects of DNA metabolism. *Bioessays* **16,** 13–22
36. Caron, P. R., Kushner, S. R., and Grossman, L. (1985) Involvement of helicase II (*uvrD* gene product) and DNA polymerase I in excision mediated by the UvrABC protein complex. *Proc. Natl. Acad. Sci. U.S.A.* **82,** 4925–4929
37. Elborough, K. M., and West, S. C. (1990) Resolution of synthetic Holliday junctions in DNA by an endonuclease activity from calf thymus. *EMBO J.* **9,** 2931–2936
38. Runyon, G. T., Bear, D. G., and Lohman, T. M. (1990) *Escherichia coli* helicase II (UvrD) protein initiates DNA unwinding at nicks and blunt ends. *Proc. Natl. Acad. Sci. U.S.A.* **87,** 6383–6387
39. Kuhn, B., Abdel-Monem, M., and Hoffmann-Berling, H. (1979) DNA helicases. *Cold Spring Harbor Symp. Quant. Biol.* **43,** 63–67
40. Kuhn, B., Abdel-Monem, M., Krell, H., and Hoffmann-Berling, H. (1979) Evidence for two mechanisms for DNA unwinding catalyzed by DNA helicases. *J. Biol. Chem.* **254,** 11343–11350
41. Matson, S. W. (1989) *Escherichia coli* DNA helicase II (*uvrD* gene product) catalyzes the unwinding of DNA·RNA hybrids *in vitro*. *Proc. Natl. Acad. Sci. U.S.A.* **86,** 4430–4434
42. West, S. C. (1997) Processing of recombination intermediates by the RuvABC proteins. *Annu. Rev. Genet.* **31,** 213–244
43. Maluf, N. K., Fischer, C. J., and Lohman, T. M. (2003) A dimer of *Escherichia coli* UvrD is the active form of the helicase *in vitro*. *J. Mol. Biol.* **325,** 913–935
44. Wessel, R., Müller, H., and Hoffmann-Berling, H. (1990) Electron microscopy of DNA.helicase-I complexes in the act of strand separation. *Eur. J. Biochem.* **189,** 277–285
45. Kaplan, D. L., and O'Donnell, M. (2002) DnaB drives DNA branch migration and dislodges proteins while encircling two DNA strands. *Mol. Cell* **10,** 647–657
46. McGlynn, P., and Lloyd, R. G. (1999) RecG helicase activity at three- and four-strand DNA structures. *Nucleic Acids Res.* **27,** 3049–3056
47. Whitby, M. C., and Lloyd, R. G. (1998) Targeting Holliday junctions by the RecG branch migration protein of *Escherichia coli*. *J. Biol. Chem.* **273,** 19729–19739
48. LeBowitz, J. H., and McMacken, R. (1986) *Escherichia coli* DnaB replication protein is a DNA helicase. *J. Biol. Chem.* **261,** 4738–4748
49. Maluf, N. K., Ali, J. A., and Lohman, T. M. (2003) Kinetic mechanism for formation of the active, dimeric UvrD helicase-DNA complex. *J. Biol. Chem.* **278,** 31930–31940
50. McGlynn, P., and Lloyd, R. G. (2002) Genome stability and the processing of damaged replication forks by RecG. *Trends Genet.* **18,** 413–419